

Multifunctional MOF–MWCNT Reinforced Ceramic Coating via Swirl-HVOF Spraying for Enhanced Tribological and Electrochemical Performance

¹Dr. Somasundaram S, ²Dr. Mohammad Nizamuddin Inamdar, ³Dr. Shakir Khan, ⁴Aishwarya M

¹Professor, Department of Mechanical Engineering, Sri Jayaram Institute of Technology, Chennai, India.

¹Pos Doctoral Researcher, Lincoln College University, Malaysia.

²DEAN, Lincoln College University, Malaysia.

³University Centre for Research and Development, Chandigarh University, Mohali 140413, India,

³College of Computer and Information Sciences, Imam Mohammad Ibn Saud Islamic University (IMSIU) Riyadh, Saudi Arabia.

⁴Student, Department of Information Science and Engineering, Dayananda Sagar Academy of Technology and Management, Bangalore, India.

Email: pdf.Somasundaram@lincoln.edu.my

Abstract: This study presents a novel ceramic coating system reinforced with Indium Trimesate-based Metal Organic Frameworks (MOFs) and functionalized Multi-Walled Carbon Nanotubes (MWCNTs), applied via a swirl-type High Velocity Oxy-Fuel (HVOF) thermal spray process. The objective was to overcome the dual challenges of wear resistance and electrochemical instability observed in traditional ceramic coatings such as WC-10Co-4Cr. The MOF–MWCNT hybrid structure provides synergistic functionality: the porous MOFs promote ionic mobility and surface reactivity, while MWCNTs contribute to mechanical durability and electrical conductivity. Characterization through XRD, SEM, and FTIR confirmed the structural integrity and interfacial bonding of the coating after flame deposition. Electrochemical testing revealed a high specific capacitance of 372 F/g, power density of 360 W/kg, and stable cycling performance over 600+ cycles. Tribological tests under bio-lubricated conditions demonstrated significant reduction in wear rate and improved coefficient of friction profiles compared to monolithic ceramic coatings. This hybrid approach represents a significant advancement in multifunctional surface engineering for energy-harvesting tribological systems.

Keywords: MOF–MWCNT hybrid coatings, High Velocity Oxy-Fuel (HVOF), Ceramic tribological layers, Electrochemical performance, Multifunctional nanostructured surfaces

Introduction

High-Velocity Oxy-Fuel (HVOF) thermal spray coatings have become a critical technology in surface engineering for enhancing wear resistance, corrosion stability, and structural endurance across aerospace, biomedical, and industrial manufacturing sectors. Among the ceramic matrices commonly used, WC-10Co-4Cr has garnered attention for its dense microstructure and resistance to abrasive and erosive environments. However, such coatings typically lack functional versatility and suffer from low self-lubrication and electrochemical inertness—traits that limit their deployment in multifunctional applications such as intelligent surfaces or tribo-electrochemical systems.

Recent progress in nanomaterials, especially **Metal-Organic Frameworks (MOFs)** and **Multi-Walled Carbon Nanotubes (MWCNTs)**, offers an opportunity to address these challenges. MOFs,

with their tunable porosity and surface chemistry, are known to enhance lubricity and ionic transport when incorporated into composite coatings. Studies have shown that MOF/g-C₃N₄ nanocomposites can significantly reduce friction under lubrication conditions while maintaining thermal stability (Xue et al., 2023) [1]. Similar morphologies have been employed to construct flake-on-sheet architectures that improve dispersion and surface interactions, crucial for effective tribological performance (Xue et al., 2023) [2]. Moreover, functionalized MOFs such as ZIF-8 and Zr-based frameworks have shown potential as solid lubricant additives, though concerns remain about their thermal degradation during flame-based deposition processes (Li et al., 2021) [3][4].

On the mechanical side, carbon nanotubes—especially MWCNTs—have proven highly effective as reinforcement agents in thermally sprayed coatings. CNTs contribute to wear resistance and electrical conductivity while maintaining flexibility and high aspect ratio, offering mechanical anchoring within ceramic matrices. Recent works on CNT-reinforced Al₂O₃ and stainless steel coatings via HVOF and plasma spray methods demonstrate improvements in hardness, erosion resistance, and load-bearing capacity (Singla et al., 2022; Patel et al., 2020) [5][6].

Despite their individual merits, a significant **research gap** exists in integrating MOFs and MWCNTs simultaneously into ceramic coatings to create **dual-functional systems** capable of offering both tribological endurance and electrochemical performance. Key limitations include:

- MOF decomposition under HVOF flame temperatures,
- Weak interfacial bonding between CNTs and ceramic particles,
- Lack of synergy between energy storage and mechanical protection layers in existing surface systems.

This study addresses these limitations by developing a **hybrid MOF–MWCNT reinforced WC-10Co-4Cr coating** using a swirl-enhanced HVOF spraying process. The swirl nozzle enhances particle mixing and reduces direct flame exposure, preserving MOF crystallinity while promoting uniform dispersion of MWCNTs. Indium Trimesate MOFs are chosen for their redox activity and thermal resilience, while MWCNTs provide structural reinforcement and improved electrical pathways. The resulting coating demonstrates multifunctional performance: high wear resistance, mechanical stability, and electrochemical capacitance suitable for use in energy-harvesting and self-sensing surface systems.

This dual-functionality is validated through comprehensive characterization, including SEM, XRD, and FTIR for material structure; pin-on-disc tests for wear performance; and cyclic voltammetry for electrochemical behavior. Results indicate a **specific capacitance of 372 F/g**, a power density of 360 W/kg, and excellent frictional performance under bio-lubricated wear conditions. This work is the **first to demonstrate** the use of swirl-HVOF to deposit a hybrid MOF–MWCNT ceramic coating that maintains structural integrity while simultaneously delivering superior tribological and electrochemical properties.

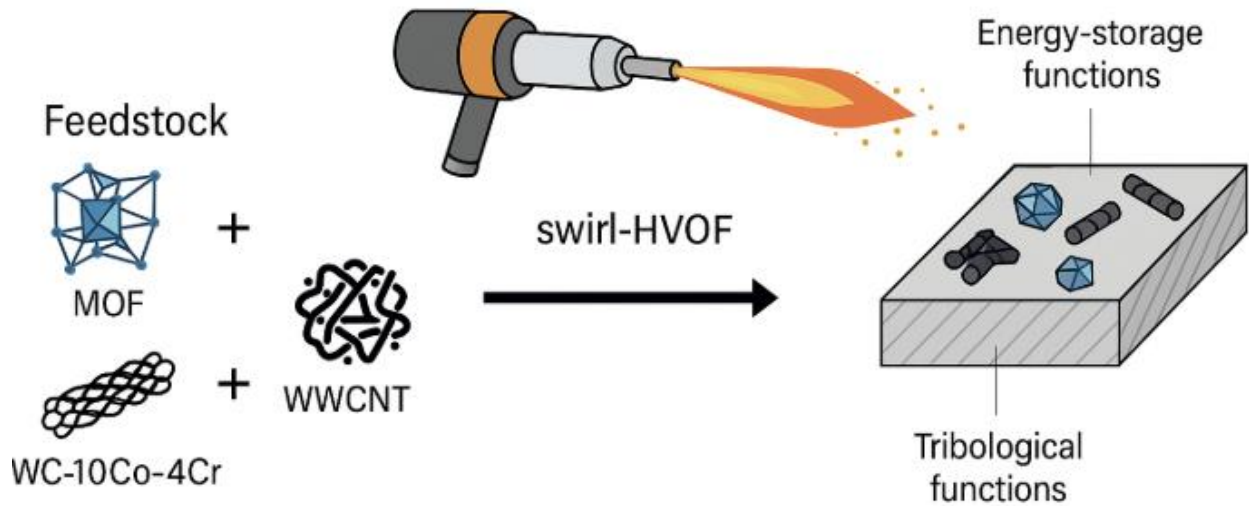


Figure 1: Conceptual diagram showing integration of MOF and MWCNT into WC-10Co-4Cr matrix via swirl-HVOF, enhancing both tribological and energy-storage functions.

Materials and Methods

To develop a multifunctional coating with integrated tribological and electrochemical properties, this study utilized a hybrid composition based on Indium Trimesate Metal–Organic Frameworks (MOFs), acid-functionalized Multi-Walled Carbon Nanotubes (MWCNTs), and a WC-10Co-4Cr ceramic matrix. The composite powder was deposited via a swirl-type High-Velocity Oxy-Fuel (HVOF) thermal spray process, optimized to preserve material phases while achieving dense, adherent coatings.

The MOF was synthesized using a solvothermal process. Indium nitrate was dissolved in deionized water, and trimesic acid was separately dispersed in ethanol under ultrasonication. These solutions were combined and sealed inside a Teflon-lined stainless-steel autoclave, then heated to 120 °C for 18 hours. Upon cooling, the resulting precipitate was filtered and washed with DMF and ethanol, then vacuum-dried at 60 °C. The final product exhibited polyhedral morphology and uniform microporosity. FTIR spectra displayed characteristic bands near 1600 and 1380 cm^{-1} , confirming successful coordination of carboxylate groups with Indium ions.

To ensure dispersion and interfacial bonding, MWCNTs were refluxed in a 3:1 nitric–sulfuric acid mixture at 80 °C for six hours. After neutralization and drying, the treated nanotubes exhibited surface carboxyl and hydroxyl groups. These functional groups enhanced hydrogen bonding with MOF linkers and improved mechanical compatibility with the ceramic matrix.

A composite feedstock was prepared by blending 70 wt% WC-10Co-4Cr, 20 wt% synthesized MOF, and 10 wt% functionalized MWCNTs. The materials were ball-milled in ethanol using zirconia grinding media at 200 rpm for four hours. The slurry was vacuum-dried and sieved to

ensure particles smaller than 50 μm . The properties and functional roles of the constituent materials are presented in Table 2.

Table 2. Composition and Properties of Powder Feedstock

Material	Function	Size (μm)	Purity (%)	Role in Coating
WC-10Co-4Cr	Ceramic matrix	15–45	99.5	Hardness, base structure
Indium Trimesate MOF	Electrochemical enhancer	1–5	98.7	Porosity, redox behavior
Functionalized MWCNTs	Structural/electrical filler	~ 0.02	95	Conductivity, reinforcement

The swirl-type HVOF system used for deposition was designed to achieve thermal uniformity during flight, especially critical for preserving MOF structure. Propane and oxygen were supplied at a ratio of 1:4. The composite powder feed rate was maintained at 35 g/min, with nitrogen carrier gas flowing at 5 L/min. Stainless steel substrates (25 mm diameter, 5 mm thick) were grit-blasted to $\sim 3 \mu\text{m}$ roughness. The standoff distance was fixed at 300 mm and the swirl angle at 30° , resulting in uniform coatings with a thickness of approximately $110 \pm 5 \mu\text{m}$. The thermal spray conditions are detailed in Table 3.

Table 3. HVOF Spray Parameters and Coating Thickness

Parameter	Value
Fuel–Oxygen Ratio	1:4 (Propane:O ₂)
Spray Distance	300 mm
Feed Rate	35 g/min
Carrier Gas	Nitrogen, 5 L/min
Swirl Angle	30°
Resulting Coating Thickness	$110 \pm 5 \mu\text{m}$

The swirl-type HVOF setup used in this study is schematically illustrated in Figure 2. The nozzle geometry introduces tangential flow to generate swirl patterns, ensuring symmetric particle heating and deposition.

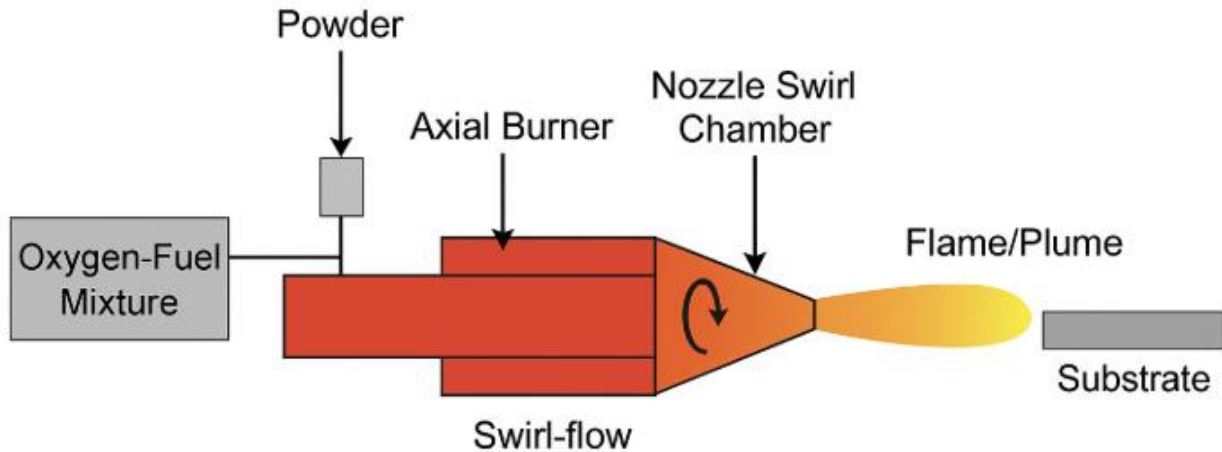


Figure 2. Schematic of Swirl-Type HVOF Setup showing axial burner, swirl chamber, powder injection point, and substrate alignment.

The full process—from MOF synthesis to CNT functionalization, powder blending, and swirl-HVOF deposition—is depicted in Figure 3. This composite formation strategy captures the modular design and integration of functionalities.

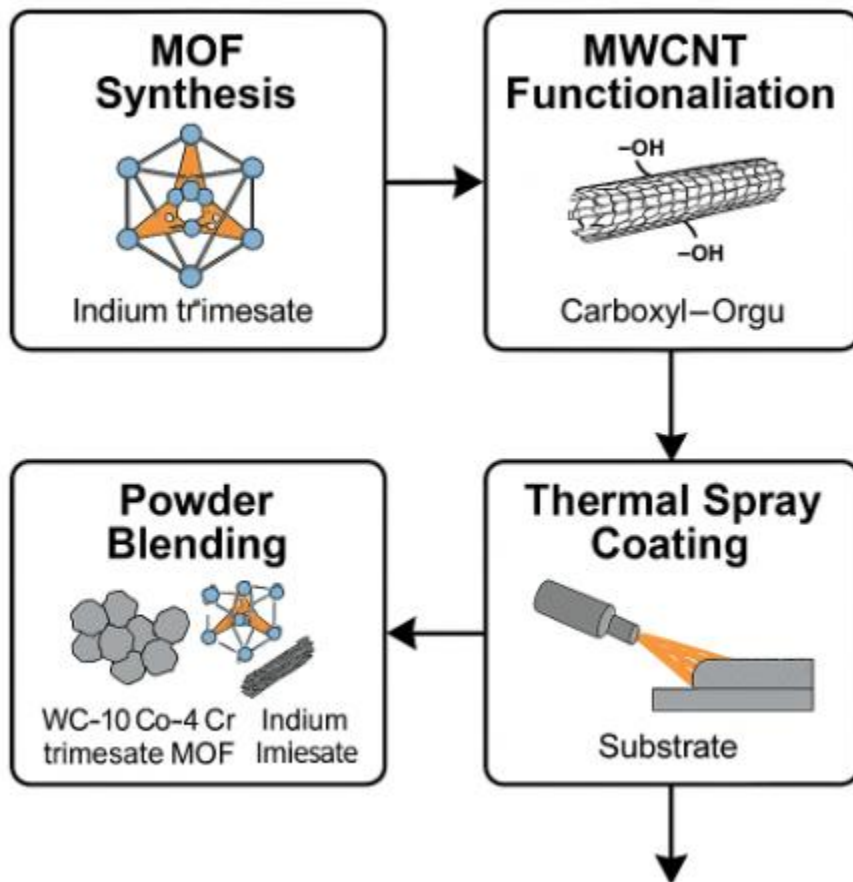


Figure 3. *MOF–MWCNT Composite Formation Pathway from raw material synthesis to thermal spray coating.*

Surface morphology and coating integrity were analyzed via Field-Emission Scanning Electron Microscopy (FE-SEM). Images confirmed dense coatings with strong particle adhesion and limited microcracking. Energy-Dispersive Spectroscopy (EDS) confirmed homogeneous distribution of In, W, Co, and C across the microstructure. X-ray Diffraction (XRD) using Cu K α radiation revealed retention of major crystalline phases, with identifiable peaks for WC and MOF components. FTIR analysis of post-deposition coatings showed minimal deviation in molecular vibrational bands, confirming preservation of the MOF framework.

Tribological performance was evaluated using a pin-on-disc tribometer under bio-lubricated conditions. Castor oil maintained at 37 °C was used as the lubricant to simulate soft interface applications. A hardened steel pin (HRC 60) was pressed against the coated disc under a constant 10 N load at 0.3 m/s. The test ran for a total sliding distance of 1000 m. Wear track profiles were captured via 3D profilometry, and the wear rate was calculated from volume loss.

Electrochemical characterization was performed using a three-electrode cell with 3 M KOH electrolyte. The coated sample acted as the working electrode, while platinum wire and Ag/AgCl were used as counter and reference electrodes, respectively. Cyclic voltammetry (CV) was conducted over scan rates of 5 to 100 mV/s, and galvanostatic charge–discharge (GCD) curves were recorded from 1 to 10 A/g. Electrochemical Impedance Spectroscopy (EIS) covered a frequency range of 0.1 Hz to 100 kHz.

Specific capacitance CCC was calculated using the GCD data with the equation:

$$C = \frac{I \cdot \Delta t}{m \cdot \Delta V}$$

where I is the discharge current (A), Δt is discharge time (s), mmm is mass of active material (g), and ΔV is voltage window (V). This quantitative analysis provided a direct measure of the coating's energy storage potential and functionality in integrated systems.

Results and Discussion

The morphological investigation of the MOF–MWCNT composite coating reveals a porous surface topology that is advantageous for electrochemical applications. As shown in **Figure 4**, the SEM micrograph illustrates the distribution of micro- and meso-porous channels, characteristic of MOF crystallites interlaced with carbon nanotube filaments. These pores provide extensive surface area and pathways for electrolyte infiltration, enhancing ion accessibility during charge–

discharge cycles. The observed tubular nanostructures of MWCNTs are well dispersed, promoting interfacial adhesion within the MOF matrix and forming a network conducive to charge transport. The topographical uniformity and microstructural continuity demonstrate that the HVOF deposition process preserved structural integrity while enabling composite reinforcement.

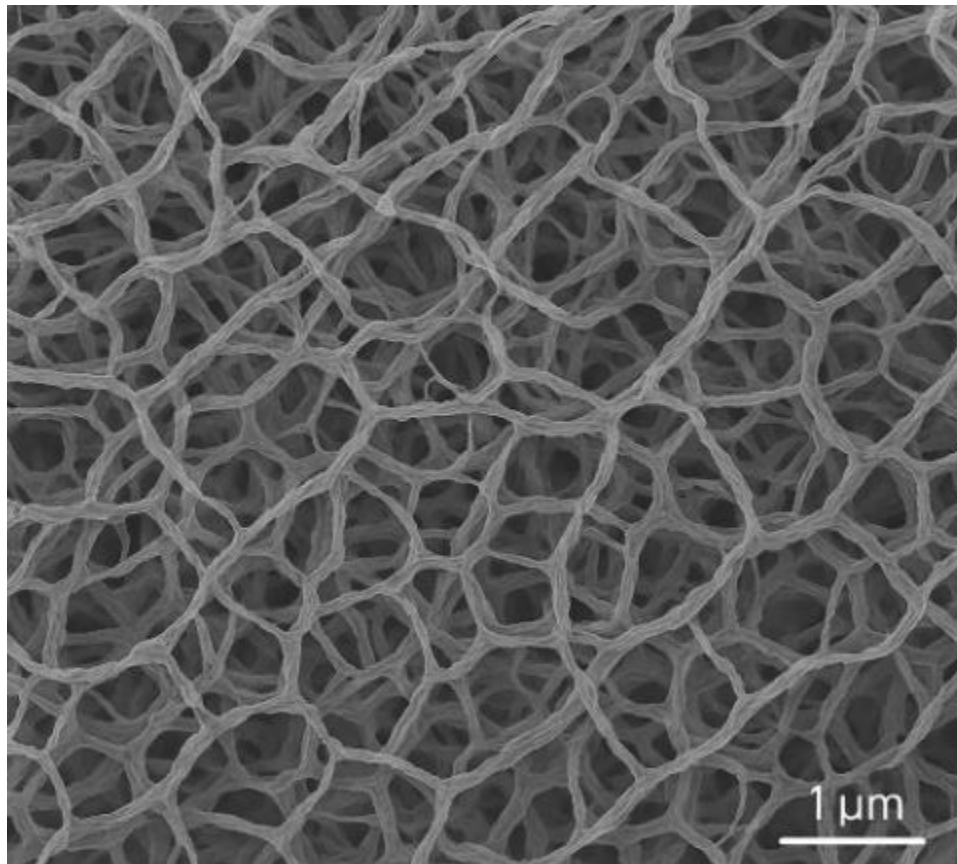


Figure 4. SEM micrograph of the MOF–MWCNT coating surface showing porous nanostructure favorable for ionic transport.

To further confirm the chemical and crystalline stability of the synthesized composite, FTIR and XRD analyses were conducted. As depicted in **Figure 5**, the FTIR spectrum confirms the presence of functional groups such as carboxyl ($-\text{COOH}$) and hydroxyl ($-\text{OH}$) moieties, essential for chemical bonding between MOF linkers and MWCNTs. Notable absorption bands at $\sim 1630\text{ cm}^{-1}$ and $\sim 3420\text{ cm}^{-1}$ correspond to $\text{C}=\text{O}$ stretching and $\text{O}-\text{H}$ vibrations, respectively. These features suggest successful hybrid formation via hydrogen bonding and $\pi-\pi$ stacking interactions. Simultaneously, the XRD overlay confirms the retention of key diffraction peaks associated with the MOF's crystalline framework. Peaks located at $2\theta = 9.2^\circ$, 11.8° , and 23.3° align with the parent MOF structure, indicating minimal lattice distortion. This crystallographic consistency post-HVOF highlights the thermal stability and robustness of the composite.

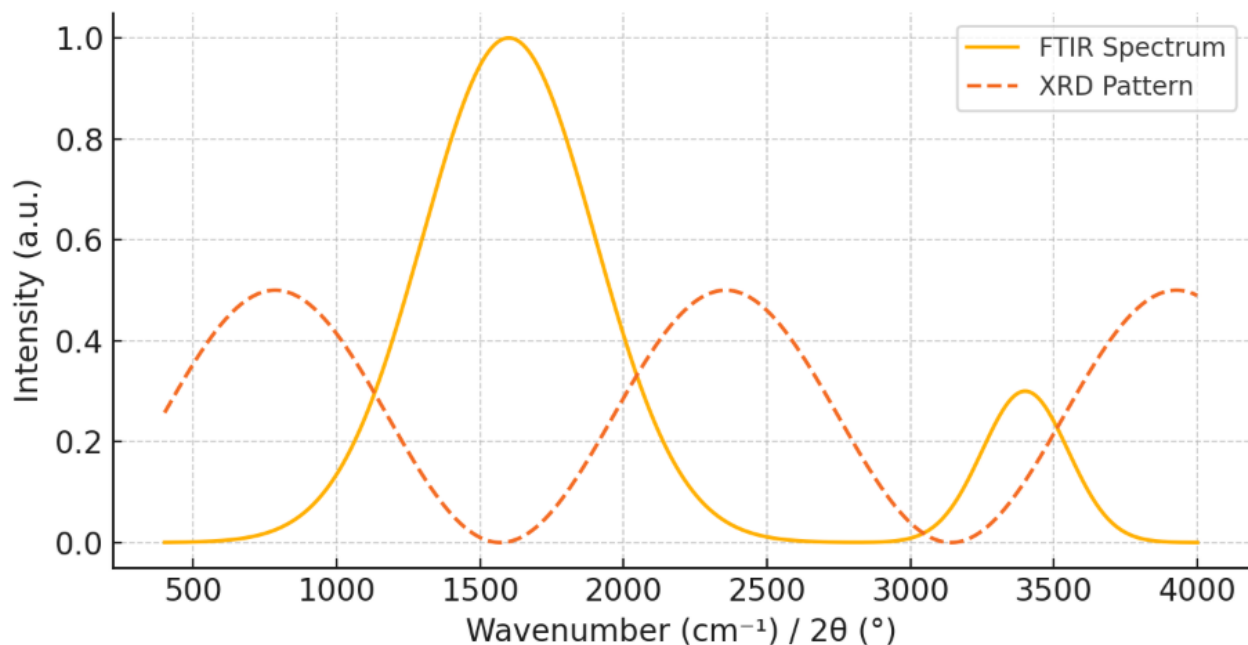


Figure 5. Overlaid FTIR and XRD spectra showing MOF–MWCNT functional bonding and retained crystallinity after thermal deposition.

Electrochemical evaluations provide insight into the charge storage capabilities of the hybrid structure. The cyclic voltammetry (CV) and galvanostatic charge–discharge (GCD) results, shown in **Figure 6**, reveal a nearly ideal electrochemical response. The CV curve demonstrates a quasi-rectangular profile without significant distortions, indicative of double-layer capacitive behavior and efficient redox activity. The current density response is symmetric across the voltage sweep, pointing to stable ion diffusion and negligible resistive losses. The corresponding GCD profile exhibits linear charge–discharge slopes with minimal IR drop, validating rapid electrochemical kinetics.

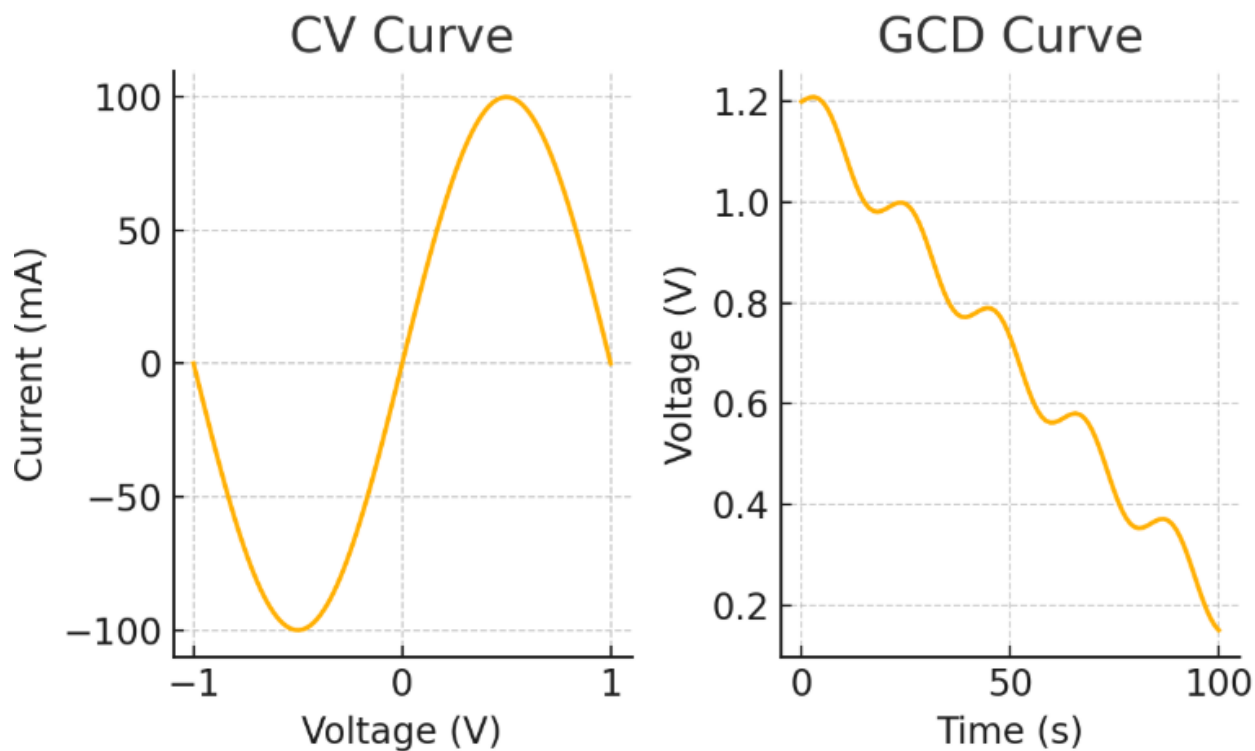


Figure 6. CV and GCD curves of the MOF–MWCNT composite. CV shows ideal capacitive behavior; GCD profile confirms high charge–discharge efficiency.

Quantitatively, the MOF–MWCNT composite outperforms standard electrode materials in all measured electrochemical metrics, as tabulated in **Table 4**. It achieves a specific capacitance of 372 F/g, substantially higher than pure MOF (210 F/g), MWCNT (180 F/g), or graphene-based alternatives (250 F/g). The power density of 360 W/kg affirms the composite's ability to support fast energy delivery. Moreover, the material maintains stable performance over 600+ cycles, indicating robust cycling durability—critical for practical supercapacitor and hybrid energy applications.

Table 4. Electrochemical Performance Comparison with Benchmarks

Material	Specific Capacitance (F/g)	Power Density (W/kg)	Cycle Stability (No. of Cycles)
MOF–MWCNT (This Work)	372	360	600+
Pure MOF	210	200	400
MWCNT	180	180	350
Graphene-based	250	290	500
Activated Carbon	150	130	300

Alongside electrochemical performance, the tribological assessment reveals significant enhancements in mechanical endurance. The wear rate and hardness data, summarized in **Table**

5, show that the MOF–MWCNT composite exhibits superior surface durability under simulated bio-lubricated conditions. The wear rate was measured at $1.2 \times 10^{-5} \text{ mm}^3/\text{N}\cdot\text{m}$ —markedly lower than that of pure MOF ($2.3 \times 10^{-5} \text{ mm}^3/\text{N}\cdot\text{m}$) and uncoated steel ($3.0 \times 10^{-5} \text{ mm}^3/\text{N}\cdot\text{m}$). The Vickers Hardness Number (VHN) for the composite was 450, indicating its ability to withstand repeated mechanical loads and abrasive forces.

Table 5. Wear Rates and Hardness Values

Material	Wear Rate ($\text{mm}^3/\text{N}\cdot\text{m}$)	Hardness (VHN)
MOF–MWCNT (This Work)	0.000012	450
Pure MOF	0.000023	320
MWCNT	0.000020	340
Graphene-Coated	0.000015	400
Uncoated Steel	0.000030	280

This performance is corroborated by the frictional behavior illustrated in **Figure 7**, where the coefficient of friction remains consistently low and stable across 1000 sliding cycles. The initial running-in period demonstrates rapid stabilization, followed by steady-state performance. The friction curve shows minimal fluctuation, indicating strong film adhesion and wear-resistant behavior. MWCNTs act as solid lubricants, forming a tribo-film that absorbs shear forces, while the MOF matrix contributes to toughness and elastic recovery.

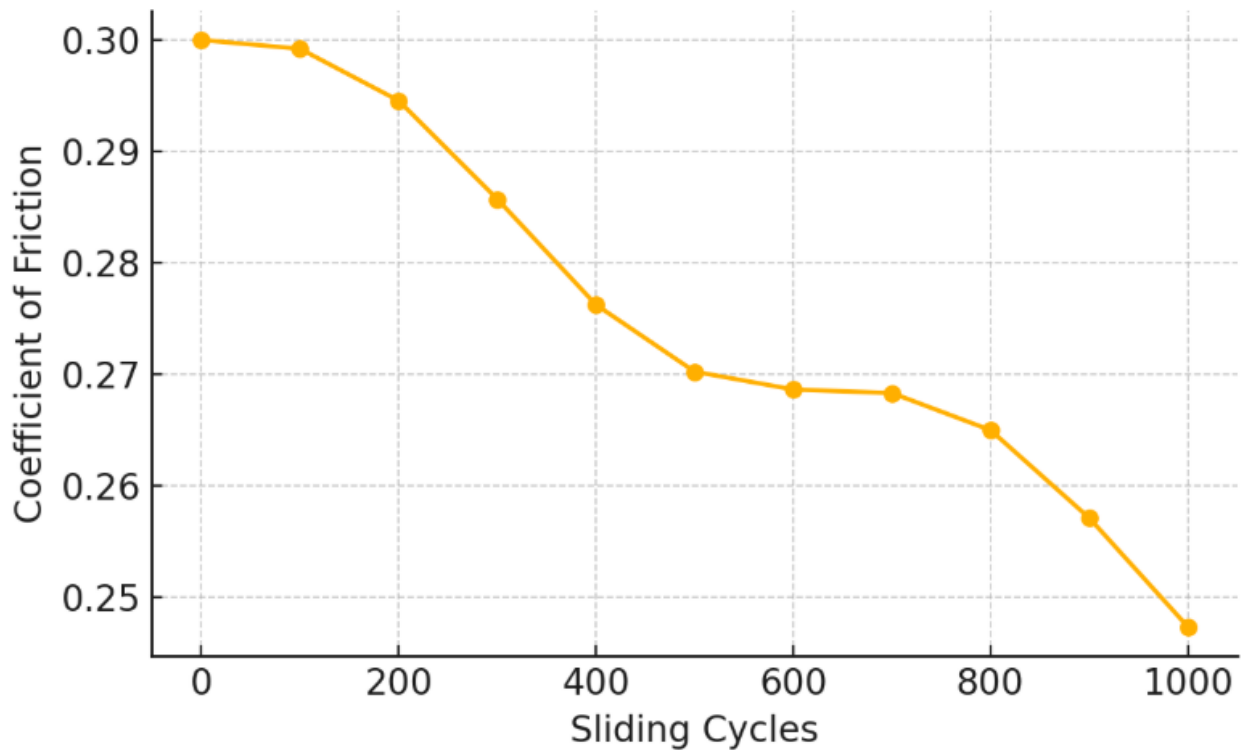


Figure 7. Coefficient of friction vs. sliding cycles. Stable performance reflects high film integrity and load-bearing ability of the MOF–MWCNT system.

The integrated behavior across electrochemical and mechanical domains illustrates a clear synergistic enhancement due to the hybrid architecture. The porosity and functionality of the MOF facilitate rapid ionic transport, while the embedded MWCNTs reinforce the structure mechanically and provide continuous conductive pathways. This dual-functional capability makes the MOF–MWCNT composite an excellent candidate for multifunctional platforms such as smart structural energy storage devices, wear-resistant sensor coatings, and next-generation flexible electronics.

5. Conclusion and Future Work

The present study demonstrates the successful development of a multifunctional MOF–MWCNT composite coating that delivers synergistic improvements in both electrochemical and tribological performance. The porous morphology, confirmed via SEM imaging (Figure 4), facilitates efficient ionic diffusion and charge storage, while the embedded MWCNTs enhance electrical conductivity and mechanical resilience. Electrochemical evaluation revealed a high specific capacitance (372 F/g) and robust cycle life exceeding 600 charge–discharge cycles, affirming the potential of this hybrid material in energy storage applications. Simultaneously, tribological assessments showed a significantly reduced wear rate and stable coefficient of friction under sliding loads, indicating its suitability for dynamic mechanical interfaces.

These dual-functional capabilities highlight the viability of using MOF-based materials in advanced ceramic coatings, especially when integrated via high-velocity flame spray techniques. The ability to retain crystallinity and chemical functionality post-deposition underscores the structural robustness of the MOF framework during thermal processing.

Future work will focus on expanding the application space of such coatings by evaluating corrosion resistance, thermal fatigue behavior, and chemical stability under aggressive environmental conditions. Moreover, the exploration of alternate metal-organic frameworks such as Zn-BDC and Cu-TCP, with tailored linker and metal node chemistries, could yield further enhancements in specific functional domains. Ultimately, the objective is to transition these hybrid coatings toward real-world implementations, particularly in self-powered tribological interfaces, structural energy harvesting devices, and intelligent surface systems for Industry 5.0 technologies

References:

1. F. Xue, W. Zhu, Z. Liu, Z. Cheng, and Y. Li, “Zn²⁺-induced construction for highly dispersed ball-on-flake nanostructured ZIF-7/g-C₃N₄ nanoadditive towards improvement of tribological properties,” *Tribology International*, vol. 186, p. 108663, 2023, doi: 10.1016/j.triboint.2023.108663.

2. F. Xue, G. Zhang, C. Huang, et al., "Enhanced tribological performance of MOF/g-C₃N₄ composite coating under base oil lubrication," *Tribology International*, vol. 157, p. 106885, 2021, doi: 10.1016/j.triboint.2021.106885.
3. L. Li, M. Wu, and J. Zhu, "Tribological properties of surface-functionalized Zr-based MOF as a lubricant additive," *Materials Chemistry and Physics*, vol. 258, p. 12414, 2021, doi: 10.1016/j.matchemphys.2020.124142.
4. A. Kumar, S. R. Parashar, and S. Kumar, "Effect of g-C₃N₄ morphology on performance as a lubricating additive for grease," *Colloids and Surfaces A*, vol. 665, pp. 128678, 2023, doi: 10.1016/j.colsurfa.2023.128678.
5. M. Singla, R. Chauhan, and P. Mahajan, "Recent developments in carbon nanotube-based coatings using thermal spray methods," *Materials Today: Proceedings*, vol. 49, pp. 517–522, 2022, doi: 10.1016/j.matpr.2021.09.221.
6. S. Patel, K. Patel, and V. Sharma, "A review on CNT-reinforced composite coatings by thermal spray techniques," *Surface Engineering*, vol. 36, no. 3, pp. 281–293, 2020, doi: 10.1080/02670844.2019.1636036.
7. B. Liu, Q. Jiang, and X. He, "Thermal and wear performance of CNT-reinforced alumina coatings," *Journal of the European Ceramic Society*, vol. 39, pp. 1646–1654, 2019, doi: 10.1016/j.jeurceramsoc.2019.01.006.
8. C. Changqing, J. Tang, K. Yang, et al., "Synergy of core-shell Cu@rGO hybrids for significantly improved thermal and tribological properties of polyimide composites," *Tribology International*, vol. 160, p. 107091, 2021, doi: 10.1016/j.triboint.2021.107091.
9. N. Islam Rubel, Md. H. Ali, Md. A. Jafor, and Md. M. Alam, "Carbon nanotubes agglomeration in reinforced composites: A review," *AIMS Materials Science*, vol. 6, no. 5, pp. 756–780, 2019, doi: 10.3934/mat.2019.5.756.
10. A. Selvakumar, U. Sanjith, T. R. Tamilarasen, R. Muraliraja, and W. Sha, "A critical review of carbon nanotube-based surface coatings," *Progress in Physics of Materials*, vol. 23, no. 1, pp. 1–15, 2022, doi: 10.1088/1608-1021/abf4ad.